Comparing dark matter models, modified Newtonian dynamics and modified gravity in accounting for galaxy rotation curves*

Xin Li(李昕)[1,2;1)] Li Tang(唐丽)[1;2)] Hai-Nan Lin(林海南)[1;3)]

[1] Department of Physics, Chongqing University, Chongqing 401331, China
[2] CAS Key Laboratory of Theoretical Physics, Institute of Theoretical Physics, Chinese Academy of Sciences, Beijing 100190, China

Abstract: We compare six models (including the baryonic model, two dark matter models, two modified Newtonian dynamics models and one modified gravity model) in accounting for galaxy rotation curves. For the dark matter models, we assume NFW profile and core-modified profile for the dark halo, respectively. For the modified Newtonian dynamics models, we discuss Milgrom's MOND theory with two different interpolation functions, the standard and the simple interpolation functions. For the modified gravity, we focus on Moffat's MSTG theory. We fit these models to the observed rotation curves of 9 high-surface brightness and 9 low-surface brightness galaxies. We apply the Bayesian Information Criterion and the Akaike Information Criterion to test the goodness-of-fit of each model. It is found that none of the six models can fit all the galaxy rotation curves well. Two galaxies can be best fitted by the baryonic model without involving nonluminous dark matter. MOND can fit the largest number of galaxies, and only one galaxy can be best fitted by the MSTG model. Core-modified model fits about half the LSB galaxies well, but no HSB galaxies, while the NFW model fits only a small fraction of HSB galaxies but no LSB galaxies. This may imply that the oversimplified NFW and core-modified profiles cannot model the postulated dark matter haloes well.

Keywords: galaxies: kinematics and dynamics, galaxies: photometry, galaxies: spiral

PACS: 95.35.+d, 98.52.Nr, 98.62.Dm **DOI:** 10.1088/1674-1137/41/5/055101

1 Introduction

It has long been found that rotation curves of spiral galaxies are significantly discrepant from the predictions of Newtonian theory [1–4]. According to Newton's law of gravitation, the gravitational force between two point-like particles is inversely proportional to the square of their separation. Therefore, the rotation velocity of a star far away from the galactic center is inversely proportional to the square root of the distance to the galactic center. However, observations often show an asymptotically flat rotation curve out to the furthest data points [5, 6]. There are several ways to reconcile this contradiction. The most direct assumption is that there is a large amount of nonluminous matter (dark matter) that has not been detected yet [7–9]. In fact, the dark matter hypothesis was first proposed to solve the missing mass problem of the sidereal system [10, 11]. However, after decades of extensive research, no direct evidence for the existence of dark matter has been found on the particle physics level. This motivates us to search for other explanations of the discrepancy between the Newtonian dynamical mass and the luminous mass.

One possible way is to modify Newtonian dynamics. In the 1980s, M. Milgrom published a series of papers to modify Newtonian dynamics in order to explain the flatness of galaxy rotation curves, which is well known today as the MOND theory [12–14]. According to MOND, Newton's second law no longer holds if the acceleration is small enough. The true dynamics should be $\mu(a/a_0)\boldsymbol{a}=\boldsymbol{a}_{\rm N}$, where $\boldsymbol{a}_{\rm N}$ is the acceleration in Newtonian theory, $\boldsymbol{a}$ is the true acceleration, and a_0 is the critical acceleration below which the Newtonian theory does not hold. The interpolation function $\mu(x)$ is chosen such that $\mu(x)\to 1$ when $a\gg a_0$, so Newton's acceleration law is recovered. In the deep MOND region $a\ll a_0$, $\mu(x)\approx x$, such that the rotation curve keeps flat at large distances from the galactic center. MOND was a non-relativistic theory for a long time until the relativistic form was constructed by Bekenstein [15]. With only one

Received 9 December 2016, Revised 18 January 2017

∗ Supported by Fundamental Research Funds for the Central Universities (106112016CDJCR301206), National Natural Science Fund of China (11305181, 11547305 and 11603005), and Open Project Program of State Key Laboratory of Theoretical Physics, Institute of Theoretical Physics, Chinese Academy of Sciences, China (Y5KF181CJ1)

1) E-mail: lixin1981@cqu.edu.cn

2) E-mail: tang@cqu.edu.cn

3) E-mail: linhn@ihep.ac.cn

universal parameter a_0, MOND has been very successful in accounting for the rotation curves of spiral galaxies [16–20].

In addition to modifying Newtonian dynamics, it is also possible to modify Newtonian gravity (MOG). According to MOG, Newton's law of gravitation is invalid at galactic scales. There are various MOG theories. Moffat [21, 22] proposed the scalar-tensor-vector gravity (STVG) and metric-skew-tensor gravity (MSTG) models, in which the gravitational "constant" is no longer a constant, but is running with distance. Carmeli [23–25] showed that the flatness of galaxy rotation curves can be naturally explained if the expansion of the universe is taken into account, and argued that dark matter may be an intrinsic property of spacetime. Horava [26–28] presented a candidate quantum field theory of gravity in $(3+1)$ dimensions of spacetime, which is known as the Horava-Lifshitz theory. Grumiller [29] proposed an effective gravity whose potential contains a Rindler term in addition to the well known terms of general relativity. All of these theories can to a large degree reconcile the missing mass problem of galaxy rotation curves.

In this paper, we make a comprehensive comparison between different models in explaining the galaxy rotation curves. We choose 9 high-surface brightness (HSB) and 9 low-surface brightness (LSB) galaxies and fit the observed rotation curves to three different types of models, i.e. the dark matter, MOND and MOG models. For the dark matter models, we choose the NFW profile [30, 31] and the core-modified profile [32] for the dark matter halo. For the MOND models, we study Milgrom's MOND theory with two different interpolation functions. For the MOG models, we focus on the MSTG theory [21]. We also compare these models with Newton's theory without adding nonluminous dark matter, denoted below as the baryonic model. Thus there are six models in total. The best model for each galaxy is picked out using statistical methods.

The outline of this paper is as follows. In Section 2, we introduce the theoretical models of galaxy structures and rotation velocities. In Section 3, we introduce the data of 9 HSB and 9 LSB galaxies that are used in our fitting. We first obtain their surface brightness parameters by fitting to the photometric data, then obtain the model parameters by fitting to the observed rotation curve data. In Section 4, we make the model comparison, and use the Bayesian Information Criterion (BIC) and the Akaike Information Criterion (AIC) to pick out the best model. Finally, discussion and a summary are given in Section 5.

2 Theoretical models

2.1 Structure of galaxies

The brightness of a galaxy is often assumed to be a direct tracer of its mass distribution. The brightness of a HSB galaxy can in general be decomposed into two components, an ellipsoidal bulge and a flat disk. The bulge is usually modeled by an inhomogeneous ellipsoid with 3D spatial brightness [33]

$$l(a)=l_0\exp\left[-\left(\frac{a}{ka_0}\right)^{1/N}\right], \tag{1}$$

where l_0 is the central density, a_0 is the harmonic mean radius of the bulge, k is a normalization factor, $a=\sqrt{R^2+z^2/q^2}$ is the distance to the galactic center, R and z are the cylindrical coordinates, q is the ratio of the minor axis to the major axis, and N characterizes the shape of the profile. Integrating over z, we obtain the 2D surface brightness of the bulge,

$$I_{\rm b}(R)=2\int_R^\infty\frac{l(a)a}{\sqrt{a^2-R^2}}{\rm d}a. \tag{2}$$

The thickness of the disk is very small compared to the galaxy size. We assume that the disk is infinitely thin, and model its surface brightness by the exponential law [34, 35],

$$I_{\rm d}(R)=I_0\exp\left(-\frac{R}{h}\right), \tag{3}$$

where I_0 is the central surface brightness in units of $M_\odot$ pc^{-2}, and h is the scale length of the disk. We can equivalently convert Eq. (3) to logarithmic units using the relation

$$\mu\,[{\rm mag/arcsec^2}]=\mathcal{M}_\odot+21.572-2.5\log_{10}I\,[L_\odot/{\rm pc^2}], \tag{4}$$

and obtain

$$\mu_{\rm d}(R)=\mu_0+1.086\left(\frac{R}{h}\right), \tag{5}$$

where μ_0 is the central surface brightness in units of mag arcsec^{-2}, and $\mathcal{M}_\odot$ and $L_\odot$ are the absolute magnitude and luminosity of the sun in a specific color-band. The total surface brightness of the HSB galaxies is given by $I(R)=I_{\rm b}(R)+I_{\rm d}(R)$. The free parameters are obtained by fitting $I(R)$ to the observed photometric data. We assume that the mass-to-light ratios of both the bulge and disk are constants.

For LSB galaxies, the surface brightness can be well approximated by the exponential disk as for HSB galaxies, while the bulge component is usually negligible [36]. However, the gas in LSB galaxies is much richer than in HSB galaxies, so it needs to be considered. The mass

profile of gas can be read from the observational data directly using the Groningen Image Processing System (GIPSY)[1)].

2.2 Models of rotation velocity

We first consider the framework of Newtonian theory. The rotation velocity induced by the spheroidal bulge can be obtained by solving the Poisson equation, and leads to the result [33]:

$$V_{\rm b}^2(R)=4\pi\sigma qG\int_0^R\frac{l(a)a^2}{\sqrt{R^2-e^2a^2}}{\rm d}a, \tag{6}$$

where G is Newton's gravitational constant, σ is the mass-to-light ratio of the bulge, and $e=\sqrt{1-q^2}$ is the eccentricity of the bulge. Similarly, the rotation velocity induced by the infinitely thin exponential disk is given by [35]:

$$V_{\rm d}^2(R)=\frac{GM}{2R}\left(\frac{R}{h}\right)^3\left[I_0\left(\frac{1}{2}\frac{R}{h}\right)K_0\left(\frac{1}{2}\frac{R}{h}\right)-I_1\left(\frac{1}{2}\frac{R}{h}\right)K_1\left(\frac{1}{2}\frac{R}{h}\right)\right], \tag{7}$$

where $M=2\pi\tau h^2I_0$ is the total mass of the disk, τ is the mass-to-light ratio of the disk, and I_n and K_n are the nth order modified Bessel functions of the first and second kinds, respectively. The rotation velocity due to neutral hydrogen (HI) can be calculated from the mass profile of HI directly using GIPSY. We assume that the mass ratio of helium (He) to HI is 1/3, and ignore other gases. Therefore, the rotation velocity contributed from the gas is given by

$$V_{\rm gas}^2=\frac{4}{3}V_{\rm HI}^2. \tag{8}$$

Then rotation velocity arising from the combined contributions of bulge, disk and gas, can be written as the squared sum of each component, i.e,

$$V_{\rm N}^2=V_{\rm b}^2+V_{\rm d}^2+V_{\rm gas}^2. \tag{9}$$

For the HSB galaxies, the gas component is negligible, hence $V_{\rm gas}=0$. For the LSB galaxies, the bulge component is negligible, hence $V_{\rm b}=0$.

There are several models for the dark mater halo, such as the NFW profile [30, 31], the pseudo-isothermal profile [37], the Burkert profile [38], the Einasto profile [39], the core-modified profile [32], and so on. All of these profiles can be generalized to the (α,β,γ)-models [40–42]. Here we focus on the NFW profile and the core-modified profile. The density of the NFW profile takes the form

$$\rho_{\rm NFW}=\frac{\rho_{\rm s}r_{\rm s}^3}{r(r+r_{\rm s})^2}, \tag{10}$$

where $\rho_{\rm s}$ and $r_{\rm s}$ are the characteristic density and scale length, respectively. The mass of dark matter, which is acquired from the volumetric integration of Eq. (10), contributes partly to the rotation curve,

$$V_{\rm s}^2=4\pi G\rho_{\rm s}\frac{r_{\rm s}^3}{r}\left[\ln\left(1+\frac{r}{r_{\rm s}}\right)-\frac{r}{r+r_{\rm s}}\right]. \tag{11}$$

Therefore, the rotation velocity in the NFW model is given by

$$V_{\rm NFW}^2=V_{\rm N}^2+V_{\rm s}^2. \tag{12}$$

The NFW profile is often quantified by the viral radius $R_{\rm vir}$ and viral mass $M_{\rm vir}$ instead of $r_{\rm s}$ and $\rho_{\rm s}$ [31, 43]. The viral radius $R_{\rm vir}$ is the radius within which the mean density of dark matter is 200 times the critical density $\rho_{\rm cr}$, and the viral mass $M_{\rm vir}$ is the mass of dark matter within $R_{\rm vir}$. These quantities are related by

$$\rho_{\rm s}=\frac{200\rho_{\rm cr}R_{\rm vir}^3}{3r_{\rm s}^3}\left[\ln\left(\frac{R_{\rm vir}+r_{\rm s}}{r_{\rm s}}\right)-\frac{R_{\rm vir}}{R_{\rm vir}+r_{\rm s}}\right]^{-1}, \tag{13}$$

$$M_{\rm vir}=200\rho_{\rm cr}\frac{4}{3}\pi R_{\rm vir}^3, \tag{14}$$

where $\rho_{\rm cr}=3H_0^2/8\pi G$ is the critical density of the universe, and H_0=70 km·s^{-1}·Mpc^{-1} is the Hubble constant.

The NFW profile is singular at the galactic center. To avoid the singularity, Brownstein [32] proposed the so-called core-modified profile. The density of the core-modified profile takes the form

$$\rho_{\rm core}=\frac{\rho_{\rm c}r_{\rm c}^3}{r^3+r_{\rm c}^3}. \tag{15}$$

The mass of dark matter within a sphere of radius r is given by

$$M(r)=\frac{4}{3}\pi\rho_{\rm c}r_{\rm c}^3\left[\ln\left(r^3+r_{\rm c}^3\right)-\ln\left(r_{\rm c}^3\right)\right]. \tag{16}$$

Thus, the corresponding rotation velocity is given by

$$V_{\rm c}^2=\frac{4}{3}\pi G\rho_{\rm c}\frac{r_{\rm c}^3}{r}\left[\ln\left(r^3+r_{\rm c}^3\right)-\ln\left(r_{\rm c}^3\right)\right]. \tag{17}$$

Therefore, the rotation velocity in the core-modified profile is given by

$$V_{\rm core}^2=V_{\rm N}^2+V_{\rm c}^2. \tag{18}$$

According to MOND theory [12, 13], Newtonian dynamics is invalid when the acceleration is approaching or below the critical acceleration a_0. The effective acceleration is related to Newtonian acceleration by

$$\mu(g/a_0)g=g_{\rm N}, \tag{19}$$

1) http://www.astro.rug.nl/∼gipsy/

where $g_{\rm N}\equiv GM/r^2$ is the Newtonian acceleration, $a_0\approx 1.2\times10^{-10}$ m s^{-2} is the critical acceleration, and $\mu(x)$ is an interpolation function which has the asymptotic behaviors $\mu(x)=x$ for $x\to0$, and $\mu(x)=1$ for $x\to\infty$. We choose two interpolation functions. The first is the standard interpolation function initially proposed by Milgrom [12]:

$$\mu_1(x)=\frac{x}{\sqrt{1+x^2}}. \tag{20}$$

Combining Eq. (19) and Eq. (20), we can solve for g,

$$g^2=\frac{1}{2}g_{\rm N}^2\left(1+\sqrt{1+\left(\frac{2a_0}{g_{\rm N}}\right)^2}\right). \tag{21}$$

Since $V=\sqrt{gR}$ and $V_{\rm N}=\sqrt{g_{\rm N}R}$, we obtain the rotation velocity in the MOND theory

$$V^2_{\rm MOND1}=\sqrt{\frac{V_{\rm N}^4}{2}+\sqrt{\frac{V_{\rm N}^8}{4}+R^2a_0^2V_{\rm N}^4}}. \tag{22}$$

Another widely used interpolation function is the so-called simple interpolation function [44]

$$\mu_2(x)=\frac{x}{1+x}. \tag{23}$$

This interpolation function can give a better fit to the Milky-Way-like HSB galaxies than the standard interpolation function [44, 45]. The corresponding rotation velocity is given by

$$V^2_{\rm MOND2}=\frac{V_{\rm N}^2+\sqrt{V_{\rm N}^4+4RaV_{\rm N}^2}}{2}. \tag{24}$$

The MSTG model was first presented by Moffat [21]. The action of the MSTG model is the Einstein-Hilbert action $S_{\rm EH}$ to which is added a mass term $S_{\rm M}$, a scale field term $S_{\rm F}$, and a term characterizing the interaction between mass and scale field $S_{\rm FM}$. In the linear weak field approximation, the MSTG acceleration law of test particles reads

$$a(R)=-\frac{G_{\rm N}M}{R^2}\left\{1+\sqrt{\frac{M_0}{M}}\left[1-\exp(-R/r_0)\left(1+\frac{R}{r_0}\right)\right]\right\}, \tag{25}$$

where $G_{\rm N}$ is Newton's gravitational constant, M is the mass of the particle, and M_0 and r_0 are characteristic parameters. The best fit to a large number of galaxy rotation curves shows that both M_0 and r_0 are approximately universal constants, i.e. $M_0\approx9.6\times10^{11}M_\odot$ and $r_0\approx13.92$ kpc [46]. Equation (25) can be regarded as Newtonian acceleration except that Newton's gravitational constant is replaced by the running gravitational "constant"

$$G(R)=G_{\rm N}\left\{1+\sqrt{\frac{M_0}{M}}\left[1-\exp(-R/r_0)\left(1+\frac{R}{r_0}\right)\right]\right\}. \tag{26}$$

Therefore, the rotation velocity in the MSTG model is given by

$$V^2_{\rm MSTG}=V_{\rm N}^2G(R)/G_{\rm N}. \tag{27}$$

3 Best-fit results

3.1 Best-fit to surface brightness

Our samples consists of 9 HSB galaxies and 9 LSB galaxies taken from published references. All 9 HSB galaxies are taken from Ref. [47], and the surface brightnesses are imaged at I-band. As for the LSB galaxies, 8 of them are imaged at R-band, and the remaining one (F730-V1) is imaged at V-band. Our samples are the same as those in Kun et al. [48]. We fit the photometric data to the models discussed in Section 2.1 using the least-χ^2 method. HSB galaxies are fitted by a bulge plus a disk, while LSB galaxies are fitted by a disk only. We list the surface brightness parameters in Table 1 and Table 2 for HSB galaxies and LSB galaxies, respectively.

Table 1. The surface brightness parameters of HSB galaxies used. The photometric data are taken from Ref. [47].

	bulge				disk	
	l_0 /($L_\odot$/pc^3)	ka_0/kpc	N	q	μ_0 /(mag/arcsec^2)	h /kpc
ESO215G39	0.7805±0.0080	0.6000±0.0027	0.6684±0.0042	0.7805±0.0080	19.3033	3.4302
ESO322G76	1.4166±0.0089	0.6272±0.0017	0.7397±0.0022	0.7082±0.0044	18.9113	2.8937
ESO322G77	5.7094±0.0103	0.1920±0.0008	1.0054±0.0030	0.5709±0.0010	18.7573	2.0541
ESO323G25	1.8523±0.0270	0.4706±0.0015	0.0212±0.0039	0.3346±0.0053	18.5259	3.0958
ESO383G02	6.3404±0.0162	0.3573±0.0004	0.7261±0.0009	0.9512±0.0024	19.7883	4.9680
ESO445G19	2.1046±0.0186	0.3723±0.0014	0.7404±0.0034	0.7368±0.0065	19.3500	4.3200
ESO446G01	1.0082±0.0019	0.6902±0.0031	1.1141±0.0030	0.8982±0.0016	19.7785	5.6008
ESO509G80	2.8310±0.0209	0.7220±0.0023	0.7049±0.0028	0.2831±0.0021	19.2745	5.4382
ESO569G17	2.8078±0.0038	0.3645±0.0011	0.7965±0.0025	0.8985±0.0012	18.2900	1.6900

Table 2. The surface brightness parameters of LSB galaxies used. The references are given in the last column.

	disk		
	$\mu_0/(\mathrm{mag/arcsec^2})$	h/kpc	Ref.
F561-1	22.39	2.60	[50]
F563-1	22.47	2.60	[49]
F568-3	22.17	3.40	[36]
F579-V1	21.90	3.80	[49]
F583-1	22.01	1.10	[49]
F730-V1	21.75	6.00	[52]
UGC128	22.38	5.10	[36]
UGC1230	22.54	3.40	[50]
UGC5750	21.80	4.20	[36]

3.2 Best-fit to galaxy rotation curves

We fit the observed rotation curve data to the theoretical models discussed in Section 2.2 using the least-χ^2 method. The best-fit parameters were obtained by minimizing the χ^2,

$$\chi^2=\sum_{i=1}^{n}\left[\frac{V_{\rm th}(r_i)-V_{\rm obs}(r_i)}{\sigma_i}\right]^2, \tag{28}$$

where $V_{\rm th}$ is the theoretical velocity, $V_{\rm obs}$ is the observed velocity, and σ is the 1σ error of $\mathrm{V_{obs}}$. In the baryonic model and MOND models, the only two free parameters are the mass-to-light ratios of the bulge (σ) and disk (τ). For LSB galaxies, $\sigma\equiv 0$, and there is only one free parameter. The critical acceleration in the MOND models is fixed at $a_0=1.2\times10^{-13}$ km$\cdot$s^{-2} [7]. In the dark matter models, there are two additional parameters, i.e. $M_{\rm vir}$ and $R_{\rm vir}$ in the NFW model, and $\rho_{\rm c}$ and $r_{\rm c}$ in the core-modified model. In the MSTG models, there are also two additional parameters, i.e. the characteristic mass M_0 and scale length r_0. However, we find that these two parameters cannot be well constrained using our galaxy sample. Therefore, we fix them to the values $M_0=9.6\times10^{11}M_\odot$ and $r_0=13.92$ kpc, which are obtained from fitting to a large sample of galaxies and taking the average [46].

The rotation curve data of HSB galaxies are taken from Palunas [47]. We list the best-fitting parameters in Table 3. We also list the reduced chi-square χ^2/dof, where dof $=N-p$ is the degree of freedom, N is the number of data points and p is the number of free parameters. For three galaxies (ESO215G39, ESO322G76 and ESO322G77) in the NFW model and five galaxies (ESO215G39, ESO322G77, ESO323G25, ESO509G80, ESO569G17) in the core-modified model, the best-fit scale parameters ($r_{\rm s}$ and $r_{\rm c}$) of the dark matter halo overstep the galaxy scale, which is physically unreasonable. The mass-to-light ratio of the disk for ESO383G02 in the core-modified model is unphysically small. Therefore, we do not list them in Table 3. For four HSB galaxies (ESO323G25, ESO383G02, ESO446G01, ESO569G17), the mass-to-light ratio of the bulge could not be well constrained in the NFW model, and we fix it to be zero. The best-fit curves accompanied by the observed data are plotted in Fig. 1. The error bars represent the 1σ uncertainty.

The rotation curve data of LSB galaxies are taken from different references. F579-V1 is taken from Blok [49], UGC128 and UGC1230 are taken from Hulst [50], and the remaining five galaxies are taken from McGaugh [51]. We list the best-fit parameters in Table 4. For all the LSB galaxies in the NFW model and three LSB galaxies (F561-1, F583-1, UGC5750) in the core-modified model, the parameters could not be well constrained. The mass-to-light ratio of disk for F568-3 in the core-modified model is unphysically small. Therefore we do not list them here. The best-fit curves accompanied by the observed data are plotted in Fig. 2, where the contributions from the gas are also shown by the black dashed curves.

4 Model comparison

To appraise which model is the best, one may adopt the most direct method by comparing the χ^2 of each model, taking the model whose χ^2 is the smallest as the best. However, a model with more parameters in general has smaller χ^2. Because the dark matter models have two more free parameters than other models, the result is not comprehensive. One may prefer to use the reduced-χ^2, i.e. the χ^2 per degree of freedom to measure the goodness of fit. We present the reduced-χ^2 in Table 3 and Table 4 for HSB and LSB galaxies, respectively. However, the reduced-χ^2 is still not comprehensive enough to evaluate the models. Therefore, in this section, we compare models with statistical analysis based on the likelihood function $\mathcal{L}=\exp(-\chi^2/2)$. One of the most used criteria to describe the goodness-of-fit is the Bayesian Information Criterion (BIC) [53],

$$\mathrm{BIC}=-2\ln\mathcal{L}_{\rm max}+p\ln N. \tag{29}$$

where N is the number of data points in the galaxy rotation curve, and p is the number of free parameters. Another widely used criterion is the Akaike Information Criterion (AIC) [54],

$$\mathrm{AIC}=-2\ln\mathcal{L}_{\rm max}+2p. \tag{30}$$

We list the χ^2, BIC and AIC values for each model in Table 5. Models with the smallest value of BIC or AIC, highlighted in boldface, are the best models. To be more visible, in Fig. 3 we plot the number of galaxies that can be best fitted by each model.

Table 3. The best-fit parameters of HSB galaxies in different models. For three galaxies (ESO215G39, ESO322G76 and ESO322G77) in the NFW model and five galaxies (ESO215G39, ESO322G77, ESO323G25, ESO509G80, ESO569G17) in the core-modified model, the best-fit scale parameters ($r_{\rm s}$ and $r_{\rm c}$) of the dark matter halo overstep the galaxy scale, which is physically unreasonable. The mass-to-light ratio of the disk for ESO383G02 in the core-modified model is unphysically small. The mass-to-light ratios of ESO323G25, ESO383G02, ESO446G01 and ESO569G17 are fixed to be zero when fitting to the NFW model. MOND1 and MOND2 stand for the MOND models with standard and simple interpolation functions, respectively.

	NFW					core				
	$\sigma_{\rm NFW}/$ $(M_\odot/L_\odot)$	$\tau_{\rm NFW}/$ $(M_\odot/L_\odot)$	$M_{\rm vir}/$ $10^{11}M_\odot$	$R_{\rm vir}/$ kpc	$\chi^2_{\rm NFW}/{\rm dof}$	$\sigma_{\rm core}/$ $(M_\odot/L_\odot)$	$\tau_{\rm core}/$ $(M_\odot/L_\odot)$	$\rho_{\rm c}/$ $(M_\odot/{\rm pc}^3)$	$r_{\rm c}/$ kpc	$\chi^2_{\rm core}/{\rm dof}$
ESO215G39	–	–	–	–	–	–	–	–	–	–
ESO322G76	–	–	–	–	–	1.25±0.12	1.35±0.10	$(0.79\pm0.23)\times10^{-2}$	13.45±4.06	0.23
ESO322G77	–	–	–	–	–	–	–	–	–	–
ESO323G25	–	0.27±0.11	6.14±0.08	173.45±8.88	0.16	–	–	–	–	–
ESO383G02	–	0.92±0.63	2.95±0.16	135.80±30.76	0.14	–	–	–	–	–
ESO445G192.13±1.64		0.38±0.75	11.81±1.68	215.66±128.57	0.08	4.29±0.67	1.96±0.13	$(0.54\pm0.23)\times10^{-2}$	17.87±14.34	0.08
ESO446G01	–	2.39±0.28	0.68±0.06	83.09±33.34	0.51	0.94±0.34	2.73±0.13	20.99±9.12	0.23±0.05	0.52
ESO509G801.25±0.60		0.71±0.47	30.85±1.98	297.01±79.68	0.20	–	–	–	–	–
ESO569G17	–	1.40±0.38	1.63±0.25	111.51±72.30	0.13	–	–	–	–	–

	baryon			MOND1			MOND2			MSTG		
	$\sigma_{\rm N}/$ $(M_\odot/L_\odot)$	$\tau_{\rm N}/$ $(M_\odot/L_\odot)$	$\chi^2_{\rm N}/{\rm dof}$	$\sigma_{\rm MOND1}/$ $(M_\odot/L_\odot)$	$\tau_{\rm MOND}{}^1/$ $(M_\odot/L_\odot)$	$\chi^2_{\rm MOND1}/{\rm dof}$	$\sigma_{\rm MOND2}/$ $(M_\odot/L_\odot)$	$\tau_{\rm MOND2}/$ $(M_\odot/L_\odot)$	$\chi^2_{\rm MOND2}/{\rm dof}$	$\sigma_{\rm MSTG}/$ $(M_\odot/L_\odot)$	$\tau_{\rm MSTG}/$ $(M_\odot/L_\odot)$	$\chi^2_{\rm MSTG}/{\rm dof}$
ESO215G39	0.43±0.24	1.81±0.05	0.36	0.79±0.18	1.21±0.04	0.16	0.58±0.14	0.86±0.03	0.17	1.26±0.19	1.24±0.03	0.20
ESO322G76	0.75±0.21	1.92±0.08	1.19	1.15±0.11	1.31±0.04	0.29	0.97±0.10	0.93±0.03	0.31	1.36±0.10	1.19±0.03	0.25
ESO322G77	1.47±0.51	3.20±0.11	0.33	1.71±0.45	2.98±0.10	0.24	1.77±0.40	2.31±0.08	0.20	2.23±0.41	2.75±0.08	0.20
ESO323G25	5.15±1.92	2.67±0.07	1.51	7.96±0.85	2.14±0.03	0.26	8.31±0.96	1.57±0.03	0.34	11.14±1.38	1.70±0.04	0.65
ESO383G02	3.23±0.33	3.05±0.07	0.17	5.56±0.52	1.70±0.11	0.36	4.55±0.39	1.13±0.08	0.31	6.69±0.48	1.26±0.10	0.50
ESO445G19	1.66±0.83	2.48±0.06	0.27	3.85±0.50	1.81±0.03	0.08	3.22±0.41	1.28±0.03	0.08	6.48±0.57	1.55±0.03	0.13
ESO446G01	2.78±0.25	2.34±0.22	1.65	3.20±0.20	1.09±0.18	1.02	2.68±0.19	0.67±0.14	1.14	3.16±0.18	0.80±0.14	1.07
ESO509G80	0.40±0.43	3.21±0.09	0.82	1.38±0.28	2.54±0.05	0.28	1.35±0.23	1.82±0.04	0.24	2.98±0.24	1.93±0.04	0.26
ESO569G17	0.12±0.21	2.10±0.06	0.19	0.16±0.16	1.87±0.05	0.11	0.34±0.16	1.40±0.05	0.13	0.50±0.16	1.71±0.05	0.13

According to the BIC criterion, one HSB galaxy (ESO383G02) and one LSB galaxy (F561-1) are best fitted by the baryonic model. Only one HSB galaxy (ESO446G01) and no LSB galaxy is best fitted by the NFW model. One HSB galaxy (ESO322G76) and no LSB galaxy is best fitted by the MSTG model. Four LSB galaxies (F579-V1, F730-V1, UGC128 and UGC1230) but no HSB galaxy are best fitted by the core-modified profile. The simple MOND model fits well for three HSB galaxies (ESO322G77, ESO445G19 and ESO509G80) and two LSB galaxies (F563-1 and UGC5750). For the remaining three HSB and two LSB galaxies, the standard MOND model is the best model.

If we apply the AIC criterion, similar conclusions can be drawn. The only difference between BIC and AIC happens in the HSB galaxy ESO323G25, which according to the BIC criterion is best fit by the standard MOND model, while according to the AIC criterion it is best fit by the NFW model. In fact, ESO323G25 can be fitted by both models very well.

5 Discussion and summary

In this paper, we have compared six different models (baryonic model, NFW profile, core-modified profile, standard MOND, simple MOND and MSTG) to account for the rotation curves of 9 HSB and 9 LSB galaxies. We fitted the observed rotation curve data to theoretical models, and used the Bayesian Information Criterion (BIC) and Akaike Information Criterion (AIC) to appraise which model is the best. We found that non of the six models can well fit all the 18 galaxies. Specifically, non of the HSB galaxies can be well fitted by the core-modified model, and none of the LSB galaxies can be well fitted by the NFW model. Only one or two (depending on whether BIC or AIC is applied) HSB galaxies are best accounted for by the NFW model. This implies that the dark matter halos, if they really exist, in some cases

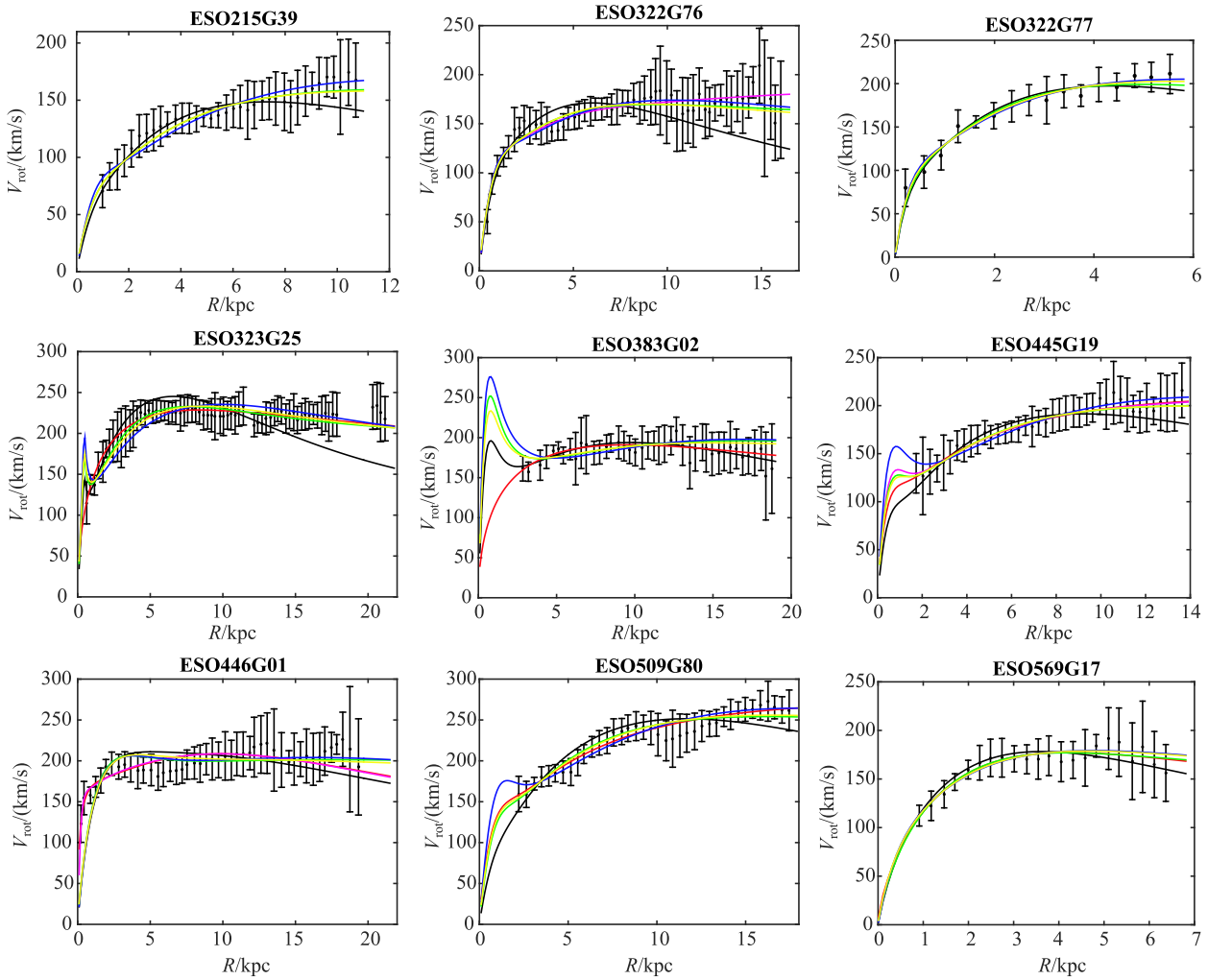

Fig. 1. (color online) The best-fit rotation curves of HSB galaxies in different models: black solid curves for the baryonic model, red solid curves for the NFW model, magenta solid curves for the core-modified profile model, green solid curves for the standard MOND model, yellow solid curves for the simple MOND model, and blue solid curves for the MSTG model. The black dots with 1σ error bars are the observed data.

Table 4. The best-fit parameters of LSB galaxies in different models. The parameters of the NFW model could not be well constrained. In the core-modified profile, the errors of mass-to-light ratios of the disk for three galaxies (F561-1, F583-1, UGC5750) overstep central values. The mass-to-light ratios of the disk for F568-3 in the core-modified model, and for F561-1 in the MOND2 model, are unphysically small. MOND1 and MOND2 stand for the MOND models with standard and simple interpolation functions, respectively.

	baryon		MOND1		MOND2		MSTG		core			
	$\tau_{\rm N}/(M_\odot/L_\odot)$	$\chi^2_{\rm N}/{\rm dof}$	$\tau_{\rm MOND1}/(M_\odot/L_\odot)$	$\chi^2_{\rm MOND1}/{\rm dof}$	$\tau_{\rm MOND2}/(M_\odot/L_\odot)$	$\chi^2_{\rm MOND2}/{\rm dof}$	$\tau_{\rm MSTG}/(M_\odot/L_\odot)$	$\chi^2_{\rm MSTG}/{\rm dof}$	$\tau_{core}/(M_\odot/L_\odot)$	$\rho_{\rm c}/(M_\odot/{\rm pc}^3)$	$r_{\rm c}/{\rm kpc}$	$\chi^2_{\rm Core}/{\rm dof}$
F561-1	2.56±0.23	0.66	0.03±0.20	11.24	–	–	1.06±1.23	26.22	–	–	–	–
F563-1	23.00±3.26	3.00	4.46±0.26	0.07	3.26±0.19	0.07	4.97±0.87	0.65	9.50±1.46	$(0.41\pm0.13)\times10^{-2}$	10.94±1229	0.08
F568-3	6.09±0.64	2.15	1.62±0.32	1.63	1.24±0.24	1.71	3.49±0.51	2.32	–	–	–	–
F579-V1	8.55±0.63	1.40	3.71±0.69	2.58	2.72±0.48	2.57	5.04±0.94	5.48	5.79±0.50	0.40±0.11	0.77±0.13	0.16
F583-1	7.12±1.51	8.43	1.50±0.43	3.36	1.19±0.37	4.35	6.03±1.79	15.46	–	–	–	–
F730-V1	7.71±0.53	1.99	4.18±0.55	2.53	3.02±0.37	2.46	5.34±0.87	8.12	5.82±0.41	0.11±0.02	1.39±0.21	0.15
UGC128	6.30±1.34	8.73	1.00±0.14	0.57	0.79±0.10	0.55	2.86±0.54	2.87	3.19±0.23	$(0.34\pm0.05)\times10^{-2}$	13.97±1.06	0.09
UGC1230	4.07±1.24	11.97	0.18±0.11	1.83	0.14±0.10	2.26	2.67±1.10	13.94	1.45±0.30	$(0.49\pm0.09)\times10^{-2}$	9.01±0.90	0.26
UGC5750	1.58±0.21	1.90	0.07±0.03	0.57	0.05±0.02	0.55	0.62±0.13	1.61	–	–	–	–

Table 5. Statistical comparison between different models. The best models are highlighted in boldface.

	χ^2_N	χ^2_{NFW}	χ^2_{Core}	χ^2_{MOND1}	χ^2_{MOND2}	χ^2_{MSTG}	BIC_N	BIC_{NFW}	BIC_{Core}	BIC_{MOND1}	BIC_{MOND2}	BIC_{MSTG}	AIC_N	AIC_{NFW}	AIC_{Core}	AIC_{MOND1}	AIC_{MOND2}	AIC_{MSTG}
ESO215G39	12.31	–	–	5.38	5.61	6.96	19.48	–	–	**12.54**	12.78	14.12	16.31	–	–	**9.38**	9.61	10.96
ESO322G76	62.97	–	11.8	15.15	16.33	13.33	70.98	–	27.8	23.16	24.34	**21.35**	66.97	–	19.8	19.15	20.33	**17.33**
ESO322G77	4.58	–	–	3.38	2.83	2.85	10.13	–	–	8.92	**8.38**	8.40	8.58	–	–	7.38	**6.83**	6.85
ESO323G25	97.85	10.38	–	16.77	22.30	42.16	106.26	27.19	–	**25.18**	30.71	50.57	101.85	**18.38**	–	20.77	26.30	46.16
ESO383G02	6.76	5.48	–	14.32	12.22	20.18	**14.24**	20.43	–	21.79	19.70	27.65	**10.76**	13.48	–	18.32	16.22	24.18
ESO445G19	10.24	2.75	2.87	3.00	2.98	4.76	17.62	17.51	17.62	10.38	**10.36**	12.14	14.24	10.75	10.87	7.00	**6.98**	8.76
ESO446G01	72.77	21.45	22.00	44.91	50.27	47.13	80.42	**36.77**	37.31	52.56	57.92	54.79	76.77	**29.45**	30.00	48.91	54.27	51.13
ESO509G80	29.51	6.70	–	10.06	8.74	9.42	36.79	21.26	–	17.33	**16.02**	16.69	33.51	14.70	–	14.06	**12.74**	13.42
ESO569G17	3.81	2.27	–	2.29	2.51	2.64	9.99	14.64	–	**8.47**	8.70	8.82	7.81	10.27	–	**6.29**	6.51	6.64
F561-1	3.97	–	–	67.41	–	157.31	**5.92**	–	–	69.35	–	159.25	**5.97**	–	–	69.41	–	159.31
F563-1	27.04	–	0.58	0.67	0.63	5.85	29.34	–	7.49	2.97	**2.94**	8.15	29.04	–	6.58	2.67	**2.63**	7.85
F568-3	21.51	–	–	16.27	17.08	23.19	23.91	–	–	**18.66**	19.47	25.58	23.51	–	–	**18.27**	19.08	25.19
F579-V1	18.25	–	1.78	33.58	33.41	71.25	20.89	–	**9.70**	36.22	36.05	73.89	20.25	–	**7.78**	35.58	35.41	73.25
F583-1	134.92	–	–	53.72	69.55	247.40	137.76	–	–	**56.56**	72.39	250.24	136.92	–	–	**55.72**	71.55	249.40
F730-V1	13.92	–	0.76	17.72	17.19	56.84	16.00	–	**7.00**	19.80	19.27	58.92	15.92	–	**6.76**	19.72	19.19	58.84
UGC128	96.06	–	0.85	6.22	6.05	31.57	98.54	–	**8.31**	8.70	8.54	34.05	98.06	–	**6.85**	8.22	8.05	33.57
UGC1230	119.73	–	2.09	18.31	22.64	139.45	122.13	–	**9.28**	20.71	25.04	141.85	121.73	–	**8.09**	20.31	24.64	141.45
UGC5750	18.96	–	–	5.75	5.53	16.06	21.36	–	–	8.15	**7.93**	18.45	20.96	–	–	7.75	**7.53**	18.06

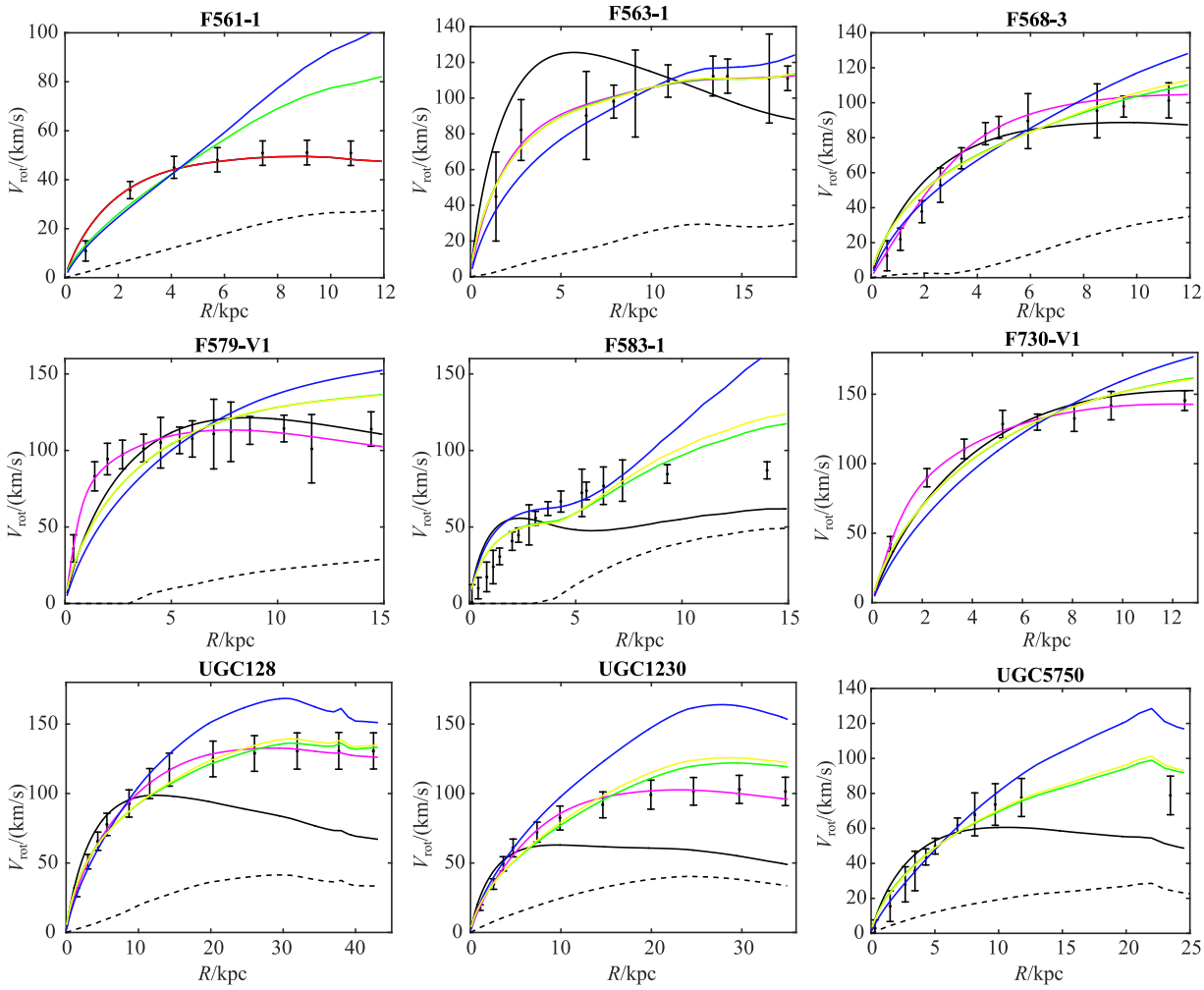

Fig. 2. (color online) The best-fit rotation curves of LSB galaxies in different models: black solid curves for the baryonic model, magenta solid curves for the core-modified profile model, green solid curves for the standard MOND model, yellow solid curves for the simple MOND model, and blue solid curves for the MSTG model. The black dots with 1σ error bars are the observed data. The black dashed curves are the contributions from the gas. Curves for the NFW model are not shown here.

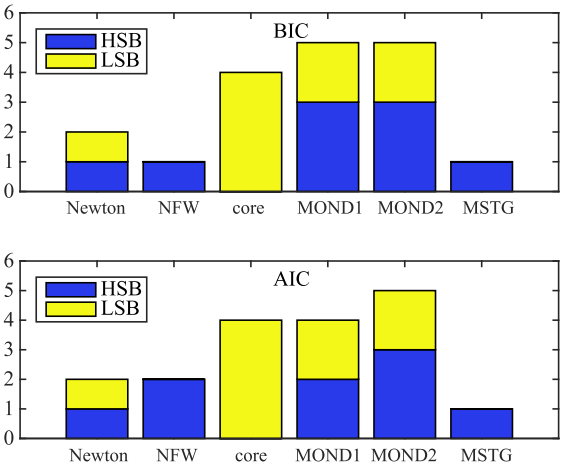

Fig. 3. (color online) The number of galaxies that can be best fit by each model. In the upper panel BIC is applied, while in the lower panel AIC is applied.

cannot be well modelled by the oversimplified NFW or core-modified profiles. Among the 18 galaxies, only one HSB galaxy can be best fitted by the MSTG model, which implies that MSTG is not a universal model. Two galaxies (one HSB galaxy and one LSB galaxy) are best accounted for by the baryonic model. For these two galaxies, it is neither necessary to add the dark matter component, nor necessary to modified Newtonian dynamics or Newtonian gravity. Two or three HSB galaxies are best fit by the standard MOND model, and three HSB galaxies are best fit by the simple MOND model. In most cases, standard MOND and simple MOND fit the data equally well. In summary, we can arrive at no convincing conclusion to prefer one model and exclude the others.

We are grateful to J. Li, H. Ma and L. L. Wang for useful discussions.

References

1 V. C. Rubin, N. Thonnard, and W. K. Ford, ApJ, **225**: L107 (1978)
2 V. C. Rubin, W. K. Ford, and N. Thonnard, ApJ, **238**: 471 (1980)
3 A. Bosma, AJ, **86**: 1825 (1981)
4 Y. Sofue and V. Rubin, ARA&A, **39**: 137 (2001)
5 F. Walter, E. Brinks, W. J. G. de Blok et al, AJ, **136**: 2563 (2008)
6 W. J. G. de Blok, F. Walter, E. Brinks et al, AJ, **136**: 2648 (2008)
7 K. G. Begeman, A. H. Broeils, and R. H. Sanders, MNRAS, **249**: 523 (1991)
8 M. Persic, P. Salucci, and F. Stel, MNRAS, **281**: 27 (1996)
9 L. Chemin, W. J. G. de Blok, and G. A. Mamon, AJ, **142**: 109 (2011)
10 J. C. Kapteyn, ApJ, **55**: 302 (1922)
11 J. H. Oort, Bulletin of the Astronomical Institutes of the Netherlands, **6**: 249 (1932)
12 M. Milgrom, ApJ, **270**: 365 (1983)
13 M. Milgrom, ApJ, **270**: 371 (1983)
14 M. Milgrom, ApJ, **302**: 617 (1986)
15 J. D. Bekenstein, Phys. Rev. D, **70**: 083509 (2004)
16 R. H. Sanders, ApJ, **473**: 117 (1996)
17 R. H. Sanders and M. A. W. Verheijen, ApJ, **503**: 97 (1998)
18 R. H. Sander and E. Noordermeer, MNRAS, **379**: 702 (2007)
19 R. A. Swaters, R. H. Sanders, and S. S. McGaugh, ApJ, **718**: 380 (2010)
20 F. Iocco, M. Pato, and G. Bertone, Phys. Rev. D, **92**: 084046 (2015)
21 J. W. Moffat, JCAP, **0505**: 003 (2005)
22 J. W. Moffat, JCAP, **0603**: 004 (2006)
23 M. Carmeli, Int. J. Theor. Phys, **37**: 2621 (1998)
24 M. Carmeli, Int. J. Theor. Phys, **39**: 1397 (2000)
25 M. Carmeli, *Cosmological Special Relativity* (Singapore, World Scientific, 2002)
26 P. Horava, PRD, **79**: 084008 (2009)
27 P. Horava, JHEP, **0903**: 020 (2009)
28 P. Horava, PRL, **102**: 161301 (2009)
29 D. Grumiller, PRL, **105**: 211303 (2010)
30 J. F. Navarro, C. S. Frenk, and S. D. M. White, Astrophys. J, **462**: 563 (1996)
31 J. F. Navarro, C. S. Frenk, and S. D. M. White, Astrophys. J, **490**: 493 (1997)
32 J. R. Brownstein, arXiv:0908.0040
33 A. Tamm and P. Tenjes 2005, A&A, **433**: 31 (2005)
34 G. de Vaucouleurs, Hdb. d. Phys, **53**: 311 (1959)
35 K. C. Freeman, ApJ, **160**: 811 (1970)
36 W. J. G. de Blok, J. M. van der Hulst, and G. D. Bothun, MNRAS, **274**: 235 (1995)
37 R. Jimenez, L. Verde, and S. P. Oh, MNRAS, **339**: 243 (2003)
38 A. Burkert, Astrophys. J. Lett., **447**: L25 (1995)
39 D. Merritt, A. W. Graham, and B. Moore et al, AJ, **132**: 2685 (2006)
40 L. Hemquist, ApJ, **356**: 359 (1990)
41 H. Zhao, Mon. Not. Roy. Astron. Soc, **278**: 488 (1996)
42 J. An and H. Zhao, MNRAS, **428**: 2805 (2013)
43 X.-F. Wu, B. Famaey, G. Gentile, H. Perets and H.-S. Zhao, MNRAS,**386**: 2199 (2008)
44 B. Famaey, J. Binney, MNRAS, **363**: 603 (2005)
45 H. S. Zhao and B. Famaey, ApJ, **638**, L9 (2006)
46 J. R. Brownstein and J. W. Moffat, ApJ, **636**: 721 (2006)
47 P. Palunas and T. B. Williams, Astrophys. J, **120**: 2884 (2000)
48 E. Kun, G. Szűcs, and Z. Keresztes et al, arXiv:1604.02465
49 W. J. G. de Blok, S. S. McGaugh, J. M. van der Hulst, MNRAS, **283**: 18 (1996)
50 J. M. van der Hulst, E. D. Skillman, T. R. Smith et al, AJ, **106**: 548 (1993)
51 S. S. McGaugh, V. C. Rubin, and W. J. G. de Blok, AJ, **122**: 2381 (2001)
52 J. H. Kim, *The Star Formation History of Low Surface Brightness Galaxies*, PhD thesis (Maryland: University of Maryland, College Park, 2007)
53 G. Schwarz, Ann Statist, 1978, **6**: 461 (1978)
54 H. Akaike, IEEE Trans. Automatic Control, **19**: 716 (1974)